ICAS-88-4.5.2

THE BEHAVIOUR AND PERFORMANCE OF LEADING-EDGE VORTEX FLAPS

D.G. Ellis * and J.L. Stollery **

College of Aeronautics, Cranfield Institute of Technology
Cranfield, Bedfordshire, U.K. MK43 0AL

Abstract

A series of low-speed wind tunnel tests were conducted on various leading-edge vortex flap (LEVF) configurations in an attempt to optimise the performance of a 60° delta wing. To describe the behaviour of LEVF's, extensive surface pressure distributions have been related to assorted flow visualisation results. The influence of the various separation and attachment lines have been clearly identified together with the effects of vortex breakdown. Results indicate that as much as 40% increase in lift-drag ratio is obtainable over a moderate lift coefficient range without any apparent loss in longitudinal stability. The additional benefits of fitting a trailing-edge flap to the vortex flapped wing are also reported.

1. Introduction

Thin slender wings with highly swept, sharp leading-edges are designed primarily for supersonic flight due to low wave drag characteristics. However, recent advances in guided missile technology have emphasised the need for improved high-speed instantaneous and sustained manoeuvrability in future combat aircraft. For delta wings with subsonic leading-edges at relatively small angles of attack, the incident freestream flow separates along the entire length of the leading edge forming a strong shear layer. The shear layer wraps up into a steady, stable vortex flow (Figure 1) which is more or less independent of Reynolds number (Ref.1).

The strength of the leading-edge vortex is normally sufficient to result in flow reattachment over the wing's upper surface. The low pressure at the core of the vortex considerably modifies the pressure distribution and gives rise to the well known non-linear lift component of the overall lift (Figure 2). This vortex-dominated flow enables the production of lift upto large angles of attack.

However, associated with the additional non-linear lift, there is a considerable drag force due to the rearward inclination of the resulting force vector (Figure 3) and the loss of leading-edge suction.

Consequently, slender wings have high lift-induced drag penalties. The performance of this class of wing them becomes far from optimal at large angles of attack, e.g. climb-to-cruise, take-off and manoeuvre. Furthermore, the utilization of vortex lift is restricted by vortex breakdown and an inherent instability in yaw, resulting in a destabilizing pitch-up tendency and large lateral forces on vertical tail surfaces respectively. (Figure 4).

In an attempt to overcome these problems and exploit the available non-linear lift, the study of vortical flows has attracted renewed interest, particularly in the context of manipulating them to the aerodynamicist's advantage.

Camber for attached flow may be introduced to alleviate the induced drag. Although this is likely to improve supersonic cruise performance (e.g. Concorde), camber for attached flow does not exploit the available non-linear lift.

An alternative device is the leading-edge vortex flap (Refs 2,3,4). The LEVF is a deflectable leading-edge control surface designed to reduce the drag of slender wings by recovering some of the leading-edge suction normally lost by the separation process. By successfully 'trapping' the vortices on the deflected flaps, a considerable forward force can be achieved on the forward facing area of the device. Furthermore, if the vortex can be manipulated such that the flow reattachment point is at the flap/wing junction, an attached lifting flow is ensured over the upper surface of the wing. (Figure 3).

A research program was initiated to validate the LEVF concept and examine the behaviour of a LEVF on a 60° delta wing. The test programme incorporated a study of the lateral stability characteristics of the LEVF configured wing and established the combined effect of LEVF and trailing-edge flaps.

2. Experimental Details

The tests were conducted in the Cranfield 2.4 m x 1.8 m low speed general purpose wind tunnel in which the freestream turbulence level was 0.09%. The 60° delta wing model tested incorporated two LEVF hinge lines running from the wing apex to 50 and 75% of the wing trailing-edge semispan† (Figure 5). Apart from illustrating flap size effects, the embodiment of two hinge lines into one model would reduce the number of model builds and facilitate an investigation of the tabbed vortex flap concept (Ref.6). To measure surface pressure distributions in the cross-flow plane, two banks of pressure tappings were set into the model at X/CR = 0.4 and 0.8. The "Scanivalve" was also located within the model to avoid excessive pressure lag effects. The leading-edges were purposely made sharp to provide a datum case with no leading-edge suction. Thereafter, any drag-reduction (i.e. 'recovered' leading-edge suction) found in the tests would be

* Research Assistant

** Professor of Aerodynamics, Cranfield Institute of Technology.

† Throughout the text the following notation is adopted. $0/50/\delta_F$ and $0/75/\delta_F$ refer to the 50% and 75% hinge locations with a LEVF deflection, δ_F, measured perpendicular to the hinge line.

a direct consequence of a favourable vortex/flap interaction.

Flap deflections (δ_F) of 0° and 60° in 5° increments were tested on both the 0/50 and 0/75 configurations. All the models were tested over an incidence range of -10° to +30° at a nominal Reynolds number of 2.0 x 10^6 per metre. Lift, drag and pitching moments were measured on the tunnel's overhead, 6-component electromechanical balance (Figure 6). The model was mounted inverted on a shielded strut, with a weighted tail sting wire for pitch atitude.

To supplement the aerodynamic force data and surface pressure measurements, smoke filament and oil-surface-flow visualisation techniques were applied to selected configurations. The optimum configuration was then equipped with a variety of trailing-edge flaps and the force measurements repeated.

All the experimental data were automatically corrected for wind tunnel balance calibration factors and wind tunnel interference corrections by the tunnel micro-computer data acquisition system.

3. Results and Discussion

Deflecting a leading-edge vortex flap on a slender wing produces an effective flap frontal area. This automatically implies changes of the aerodynamic forces and moments acting on the configuration. The performance benefits (i.e. increases in lift-drag ratio) are expected to arise when the leading-edge vortex is 'trapped' entirely on the flap so that reattachment (A1, Figure 1) coincides with the wing/flap junction. This provides a forward force (thrust) due to the vortex suction acting on the forward facing area of the deflected flap. During the process of optimising the performance of LEVF, variable flap deflection provides the simplest means of altering the flap's performance characteristics. Clearly, the optimum flap deflection (maximum L/D increase) will depend on the wing's angle of attack which in turn governs the local leading-edge flow upwash. The deflection should be as large as possible to maximise thrust, yet not so large as to prevent separation at the flap leading-edge and hence avoid vortex formation. This situation will arise if the local flow upwash at the flap leading-edge matches the flap deflection. Depending on the value of the flap deflection at a given wing incidence, separation will occur over the top surface of the flaps or at the flap/wing junction or on the underside of the flap.

In order to concentrate on the true aerodynamic affect of flap deflection, all the aerodynamic data were reduced to coefficient form, based on the planform area of the datum configuration. Consequently, the aerodynamic data for the planar configuration provides a basis for comparison. Many of the previous studies which involved increases of planform area due to the addition of LEVF provided falsely optimistic results because the area increase was not included when defining the aerodynamic coefficients. The added area of the flaps will obviously increase the wing's lift and drag while aerodynamic changes caused by the movement of the leading-edge vortex from the wing to the flap should reduce its drag and possibly it's lift. Lift increases (and drag changes) occurring simply because of the added area of the flaps cannot appear in the C_L-C_D data of the present tests.

Since it is impossible to show all the data in this paper, selected results which illustrate the salient features of LEVF aerodynamics are presented and discussed. A more comprehensive analysis of the results can be found in Ref.10.

The essential aerodynamic effects of flap deflections (δ_F = 0°, 10°, 20°, 30°, 40°, 50°, 60°) on both the 0/50 and 0/75 configurations are assessed from the graphs of C_L - α, C_D - α and C_m - C_L (Figures 7-9). It is evident that for all LEVF configurations at a given incidence, increasing flap deflection produces a decrement in C_L. However, the decrement for a given flap deflection is less so in the case of the 0/75 configurations (Figure 7). Consider the planar configuration at a moderate incidence. Introducing a mild flap deflection will alter the effective leading-edge upwash and hence the strength of the resulting separated vortical flow. Furthermore, since the flap deflection provides an effective forward facing area, the vortex suction force is tilted out of the normal plane. Further increasing the flap deflection lessens the vortex strength since the local upwash, αu, approaches δ_F, until in the limiting case, the flow attaches at the flap leading-edge and separates at the flap/wing junction. A further increase in δ_F results in the flow separating on the underside of the flap. The situation is further complicated by the fact that the local flap leading-edge upwash is not constant along the entire length of the leading-edge.

The stall of the datum wing is characterized by a gentle turning over of the C_L - α curve as the vortical flow field (which in turn controls flow reattachment and hence the potential lift) is gradually destroyed by the action of vortex breakdown.

The primary benefit accrued from LEVF's is a reduction of drag (2,3,4). For lift coefficients above 0.2, the suction developed by the flap bound-vortex produces a thrust. This appears as a reduction in C_D for increasing flap deflection at a given wing incidence for both the 0/50 and 0/75 configurations (Figure 8). The reduction in C_D for a given flap deflection is greater for the 0/50 configurations since the larger flap provides a greater forward facing area on which the redirectioned vortex suction force can act. Consistent with the increase of the zero lift incidence for increasing flap deflection (Figure 7), the incidence for minimum drag also increases for increasing δ_F (Figure 8).

Pitching moments were measured about the model mounting point which was at 40% of the wing centreline chord measured from the wing apex (Figure 6). The effect of flap deflection on the pitching moment coefficients for the 0/75 configuration is illustrated in (Figure 9). The slope of the C_M - C_L curve gives a direct measure of the centre of pressure position of each of the configurations. The results clearly indicate that flap deflections have very little effect on the longitudinal stability of the LEVF configured wings. One surprising feature of the pitching moment characteristics is the absence of any noticeable 'kink' in the C_M - C_L curve due to the loss of non-linear vortex lift as the vortex breakdown position crosses the wing trailing-edge. The 'kink' would be more noticeable on a wing of greater leading-edge sweep which would provide stronger leading-edge vortices.

The relative changes of lift and drag due to LEVF deployment will dictate the overall effect on lift-drag ratio. It is apparent from Figure 10 that a 30° flap deflection on the 0/75 configuration (0/75/30) offers a peak L/D improvement of 40% at a lift coefficient of 0.45. As the wing camber increases (increasing δ_F), the value of C_L at which the LEVF benefit is first obtained also increases. On the basis of the results in Figure 10, the 0/75/30 configuration was considered as the performance-optimised LEVF configuration.

The effect of 0/75 flap deflection on the spanwise pressure distribution at various fixed wing incidences is shown in Figure 11. The data is presented in the form of pressure coefficient versus the non-dimensionalized wing semispan and pertains to the wing upper surface only, at x/C_R = 0.4. The wing/flap junction is located at η = 0.75. At an incidence of 6°, increasing flap deflection results in a gradual collapse of the

leading-edge vortex. The flow attaches at the flap leading-edge for a flap deflection of 30°. Thereafter, a further increase of flap deflection causes the flow reattachment line to move over the upper surface towards the wing/flap junction. An extreme deflection of 60° results in a wing/flap junction separation on the wing upper surface. The measured lower surface pressure distributions illustrate large extents of separated flow for flap deflections greater than 30°. The situation at 6° incidence is magnified at a wing incidence of 12°. The flap deflection for attached flow at the flap leading edge is increased ($50° < \delta_F < 60°$). The flap/wing junction separation is strengthened. Increasing the wing incidence (α = 18°, 24°) increases the peak suction levels and causes the primary attachment line to move progressively inboard.

The combined effect of LEVF's and trailing-edge flaps is illustrated in Figure 12. For lift coefficients above 0.5, trailing-edge flap deflections of 10°, 20° and 30° all offer increased L/D ratios compared with the 0/75/30 configuration with no TEFs. The significant performance improvements at the higher lift coefficients are due to the susceptability of the leading-edge vortex flow to increased upwash angles and the increased circulation induced by the trailing edge flap.

A brief study was conducted in the college's hydrodynamic facility to establish the effect of LEVF on the vortex breakdown phenomenum. The results are illustrated in Figure 13.

It is generally assumed that separated vortex flows where primary separation occurs at a sharp leading-edge are relatively insensitive to Reynolds number (Ref.7). This assumption provides the justification for flow visualisation tests in water at Reynolds numbers in the range 1000 - 20000, as compared to wind tunnel tests at typically 2×10^6. The results illustrate a delay in vortex breakdown when LEVF are deployed. This effect is directly attributable to a sweep effect since deploying LEVF results in an increased effective sweep and hence a reduction in susceptability of the leading-edge vortex to burst phenomena.

In an attempt to identify the various attachment and separation lines associated with LEVF configured wings, various surface flow visualisation photographs were taken. A typical example is shown in Figure 14. The primary attachment lines (A1, Figure 1) are clearly identifiable just outboard of the wing centreline. Regions of secondary separation can also be identified as two black streaks between X/C_R = 0.2 and 0.4 on the flap surfaces.

4. Comparisons with Theory

The primary theoretical approach adopted in the analysis of thin, slender delta wing planforms is that due to Polhamus (5). The Polhamus leading-edge suction analogy is based on the supposition that the attached flow leading-edge suction is rotated through a right angle and hence provides a normal force contribution in the separated flow case. Neglecting viscosity, the resultant force acting on the wing is then the sum of the rotated leading-edge suction force and the potential lift due to attached flow with zero leading-edge suction. Consequently, the method provides quick estimates of the overall aerodynamic forces and moments acting on slender wings which are dominated by separated flows. A comparison between the experimental data and the suction-analogy prediction for the 60° planar delta wing is shown in Figure 15. Vortex bursting normally begins to limit vortex lift at an angle of attack of about 15° on a 60° delta wing (Figure 13) and finite wing thickness (and hence surface curvature) also tend to reduce vortex lift. Consequently, the suction analogy, which assumes zero wing thickness and no vortex bursting, is unable to predict the results for the 60° wing above an incidence of 15°.

Figure 16 illustrates the amount of leading-edge suction recoverable through LEVF deployment. Taking first the simplest case of a plane, uncambered and untwisted wing, aspect ratio AR, and assuming that, in the absence of any flow separations;

$$C_D = C_{Do} + KC_L^2/\pi\, AR$$

where C_{DO} is the zero-lift drag and relates to the surface skin friction and form drag, and C_{Di} ($= KC_L^2/\pi AR$) is the lift-induced or vortex drag for attached flow with 100% leading-edge suction, the lift-drag ratio is then given by;

$$L/D = \left\{ C_{Do}/C_L + KC_L/\pi\, AR \right\}^{-1}$$

On the other hand, the maximum drag limit in the complete absence of leading-edge suction corresponds to:

$$C_D = C_{Do} + C_L \tan \alpha$$

Using a value of K = 1 and C_{Do} = 0.006, the 0% LE suction and the 100% LE suction boundaries are plotted in Figure 16. The experimental results for the optimum 0/75/30 configuration illustrate the recoverable leading-edge suction.

Figure 17 compares the experimental results for the 0/50/30 and 0/50/60 configurations with an extended suction-analogy method due to Hardy and Fiddes (8). The calculation method is summarized below:-

(a) Using the SPARV three-dimensional panel method (9) the contribution of each section of the leading-edges to the suction force was calculated and rotated to act normal to the local plane of the wing at the edge (consistent with Polhamus approach).

(b) The resulting force was then resolved to give lift and drag increments associated with separated flow via the suction analogy.

(c) SPARV was used to calculate attached flow forces in the absence of any leading-edge suction. The total lift and drag forces were then obtained by adding the separated flow contributions to the attached flow components.

Although the overall trends are predicted (i.e. large lift loss and small drag reduction), the lack of quantitative agreement is due to the fact that the grossly non-planar configurations presented some difficulty in modelling within the SPARV program. The non-streamwise hinge-line necessitated the use of non-streamwise panelling which leads to some loss of accuracy within the panel method.

5. Conclusions

The test series revealed that the 0/75/30 configuration can offer as much as a 40% increase in L/D with a considerable improvement over a moderate lift coefficient range. The deployment of LEVF's has no effect on the longitudinal stability characteristics of the configuration. The combined use of LEVF and trailing edge flaps offers additional benefits in lift-drag ratio. The primary benefit accrued from LEVF's is a drag reduction

due to the effective recovery of the lost leading-edge section for separated flow. Theoretical predictions based on Polhamus' suction analogy successfully illustrate the mechanism by which LEVF's improve overall aerodynamic performance.

6. References

1. Henderson, W.P. — Studies of various factors affecting drag due to lift at subsonic speeds. NASA TN D - 3584, October 1966.

2. Marchmann, J.F. — Effectiveness of leading edge vortex flaps on 60 and 75 degree delta wings. Journal of Aircraft, Vol 18, No.4. April 1981.

3. Reddy, C.S. — Effect of leading-edge vortex flaps on the aerodynamic performance of delta wings. AIAA paper 81 - 4236 (1981)

4. Rao, D.M. — Leading edge vortex flap experiments on a 74 degree delta wing.

5. Polhamus, E.C. — A concept of the vortex lift of sharp-edged wings based on a leading-edge suction analogy. NASA TN D-3767, December 1966.

6. Hoffler, K.D. Rao, D.M. — An investigation of the tabbed vortex flap. AIAA-84-2173

7. Thompson, D.H. — A visualisation study of the vortex flow around double-delta wings ARL-AERO-R-165, 1985

8. Hardy, B.C. Fiddes, S.P. — Prediction of vortex lift of non-planar wings by the leading-edge suction analogy. Aeronautical Journal, April 1988.

9. Petrie, J.A.H. — A surface source and vorticity panel method. Aeronautical Quarterly, 1978,29, pp 251-269.

10. Ellis, D.G. — The Behaviour and Performance of Leading-Edge vortex flaps. Cranfield Institute of Technology, Ph.D. Thesis (To be published).

7. Nomenclature

AR	aspect ratio
α	incidence (degrees)
B	wing semispan
C	wing chord
C_D	drag coefficient
C_{Do}	zero-lift drag coefficient
C_L	lift coefficient
C_{Lmax}	maximum lift coefficient
C_M	pitching moment coefficient (about $X/C_R = 0.4$)
C_P	pressure coefficient
C_R	wing root chord
δ_F	flap deflection (degrees, perpendicular to hinge-line)
F	aerodynamic force
K	lift-induced drag factor
L/D	lift-drag ratio
U_∞	freestream velocity
x, X	axial distance measured from wing apex
y, Y	spanwise distance measured from wing centreline
η	non-dimensionalized semispan location (= 2Y/B)
Λ	leading-edge sweep angle

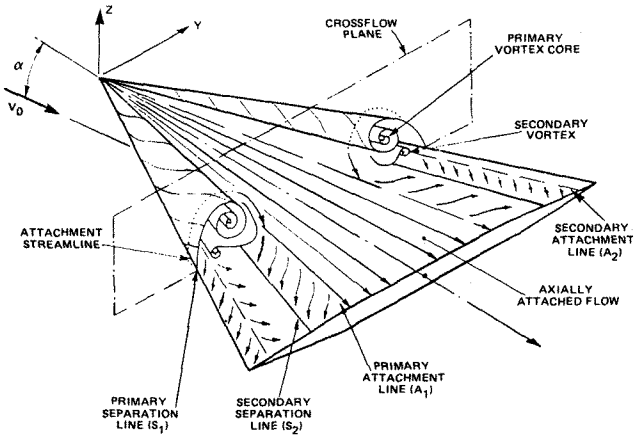

Figure 1 Sharp-Edged Delta Wing Flow

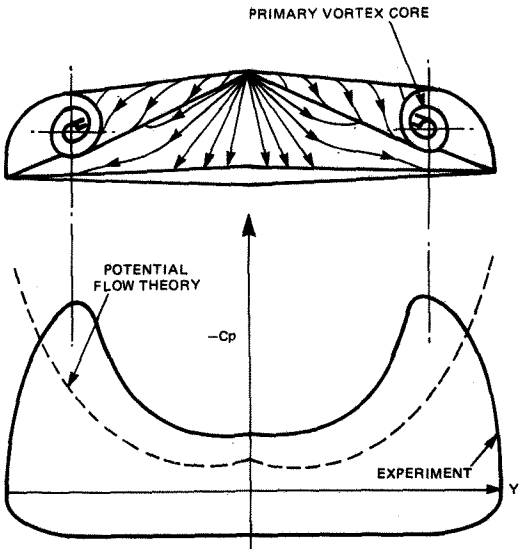

Figure 2 Cross-Flow Plane Pressure Distribution

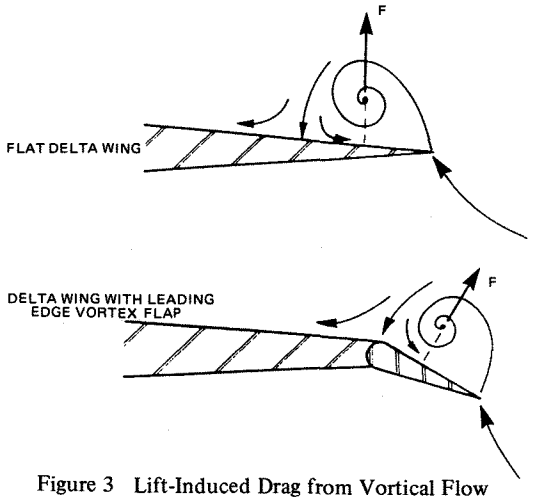

Figure 3 Lift-Induced Drag from Vortical Flow

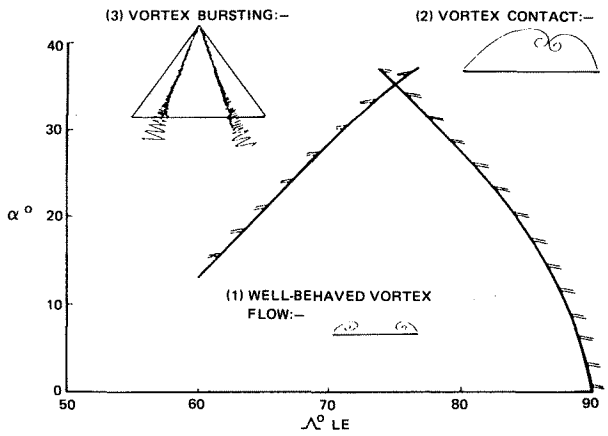

Figure 4 Slender Wing Flow Boundaries

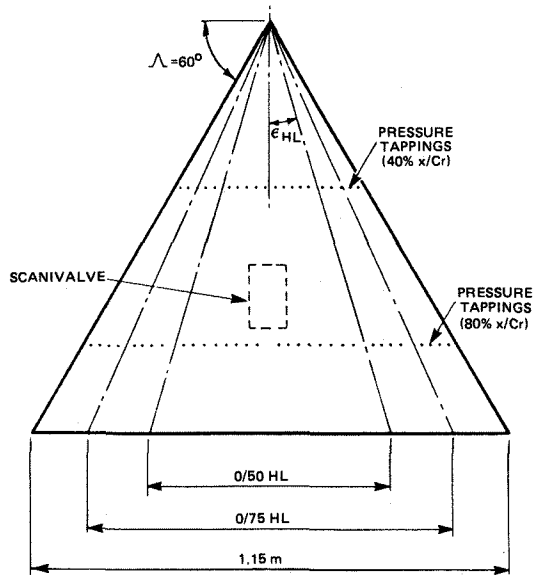

Figure 5 LEVF Research Model Details

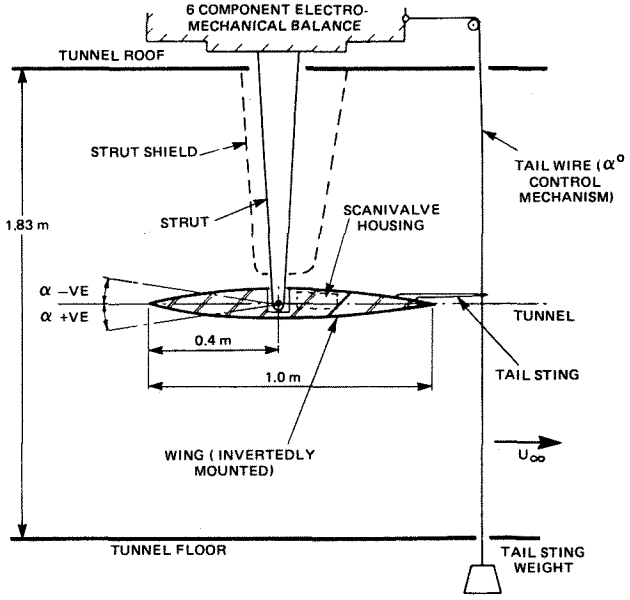

Figure 6 Wind Tunnel Model Mounting Details

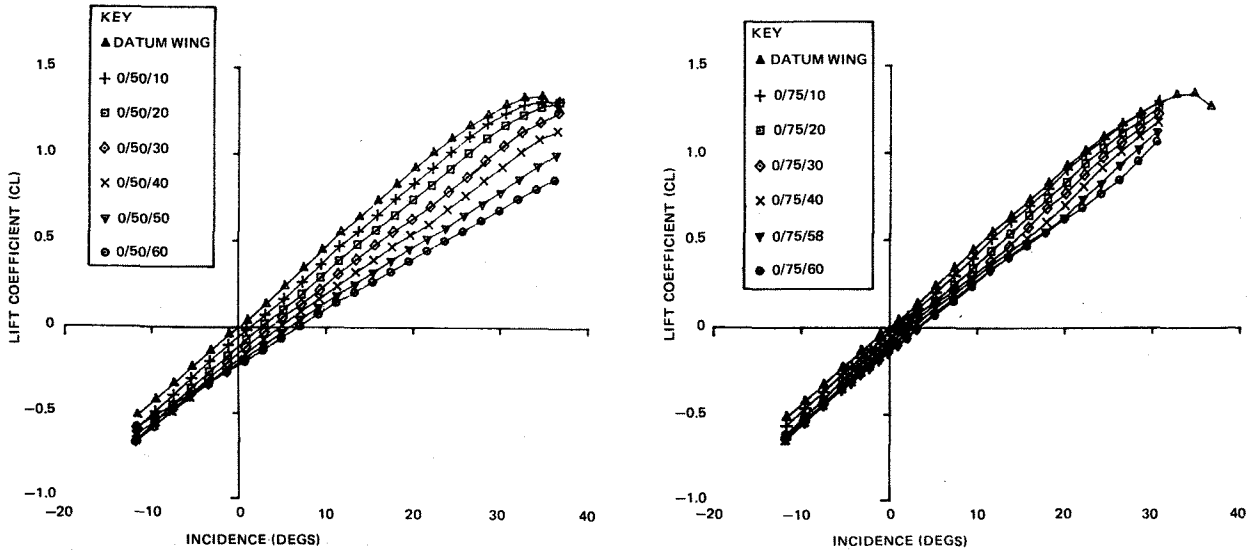

Figure 7 The Effect of Flap Deflection of Lift Coefficient

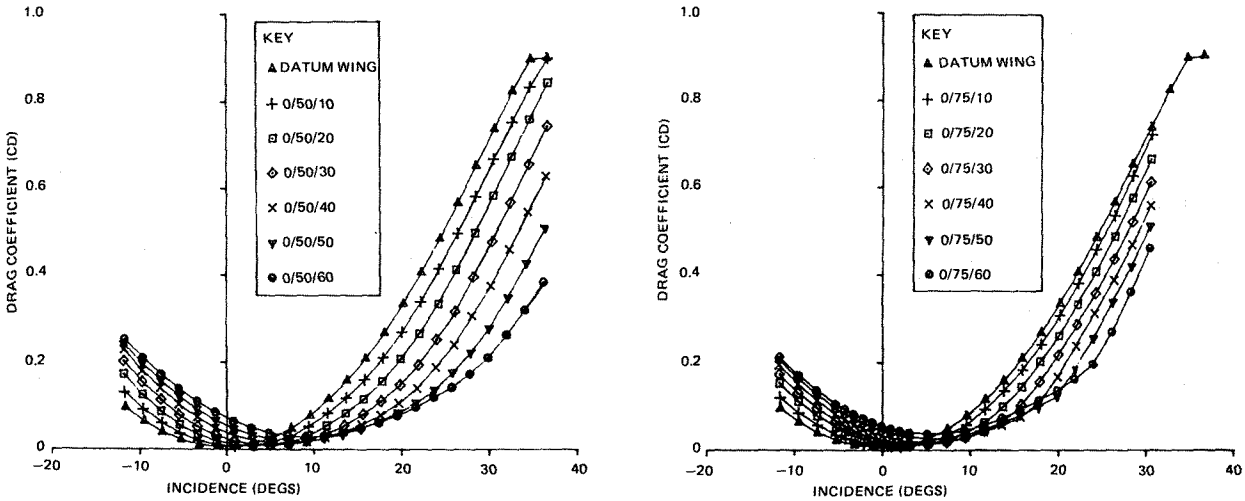

Figure 8 The Effect of Flap Deflection on Drag Coefficient

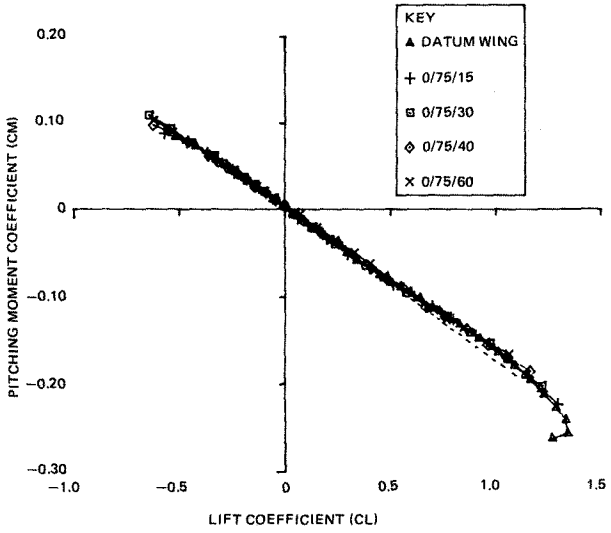

Figure 9 The Effect of Flap Deflection on Pitching Moment Coefficient

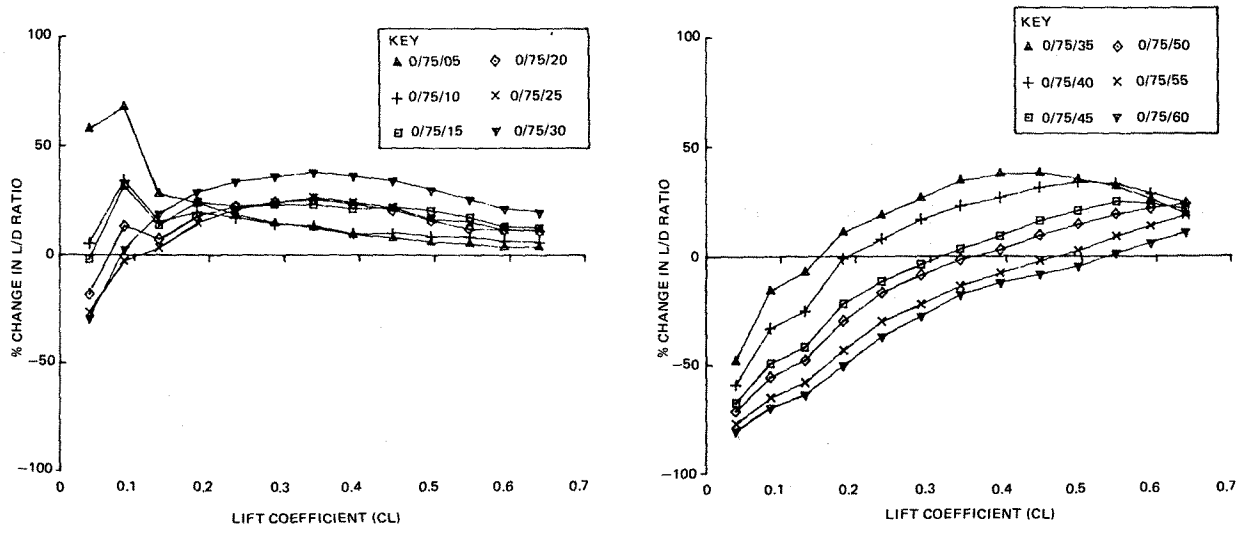

Figure 10 Improvements in L/D Due to LEVF

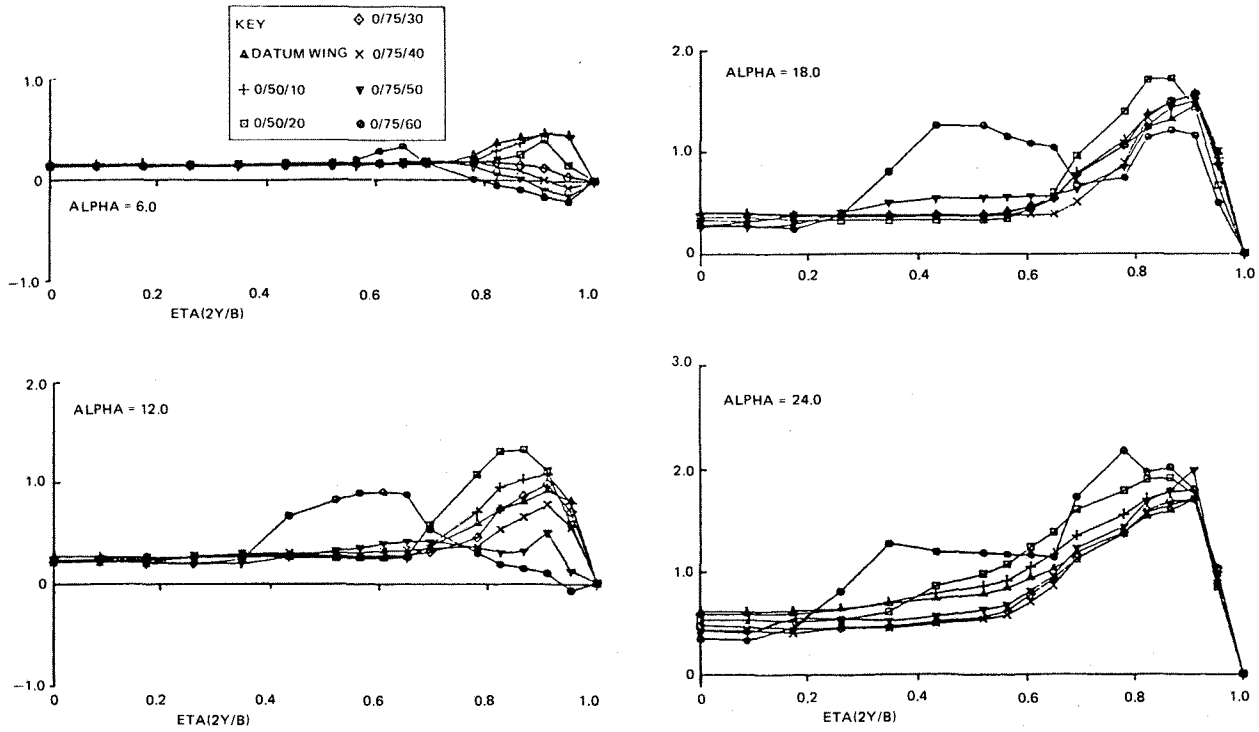

Figure 11 Effect of Flap Deflection on Cross-Flow Pressure Distribution

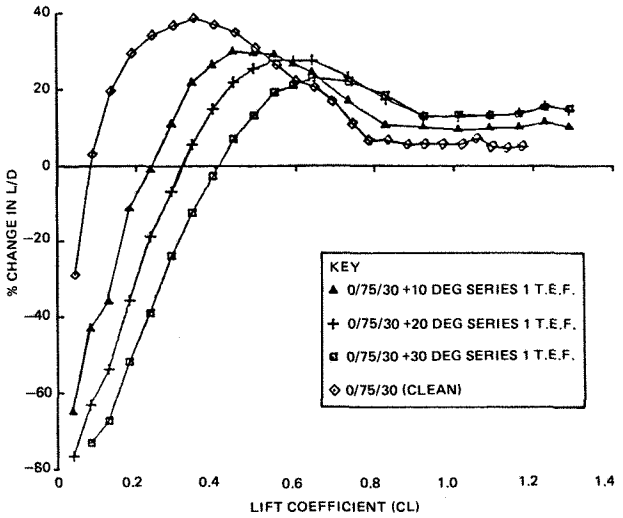

Figure 12 Combined Effect of LEVF and Trailing Edge Flaps on L/D

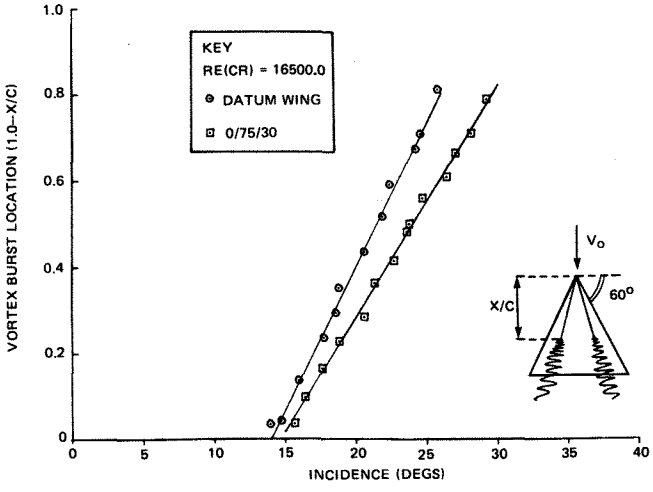

Figure 13 Effect of LEVF on Vortex Breakdown

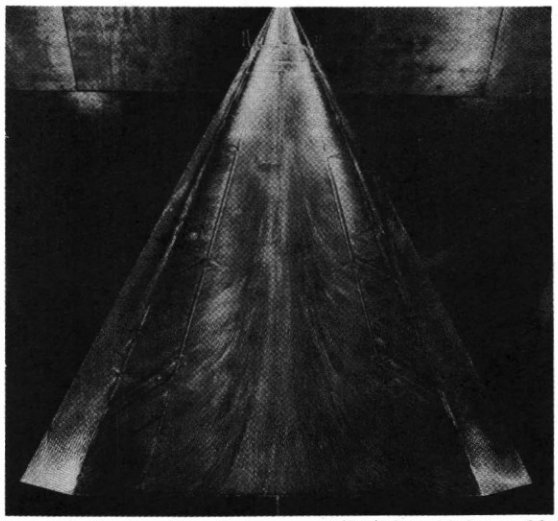

Figure 14 Surface Flow Pattern on 0/75/30 at Alpha = 30.0

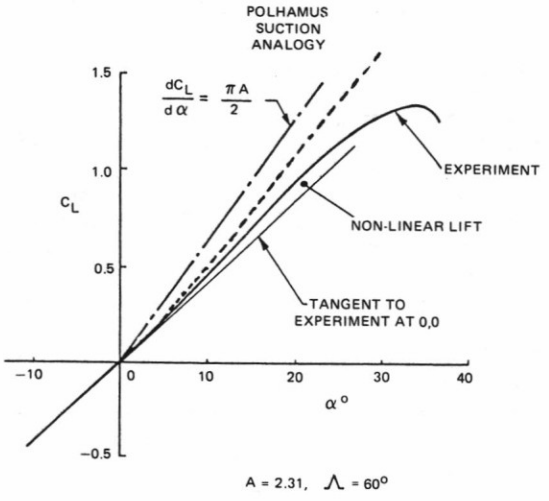

Figure 15 CL Versus Incidence-Experiment and Theory

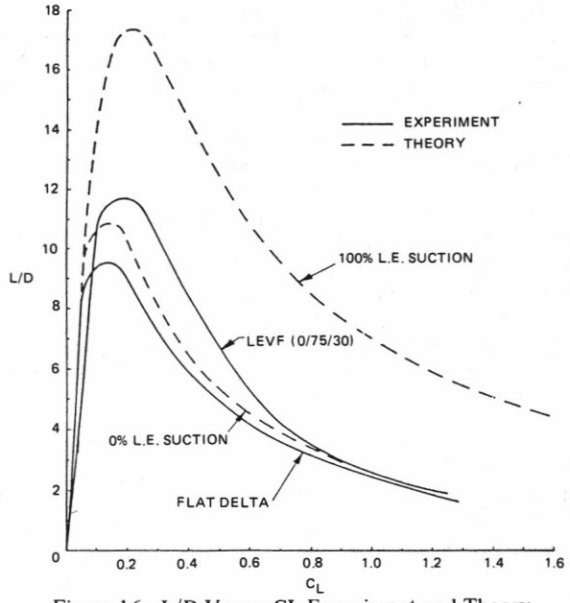

Figure 16 L/D Versus CL-Experiment and Theory

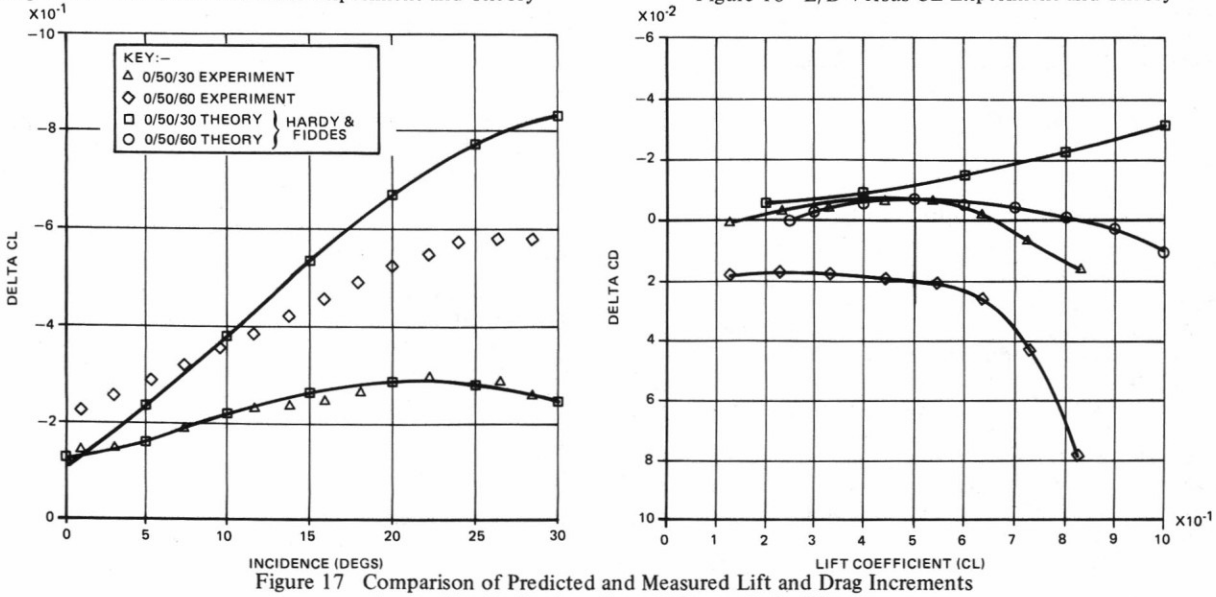

Figure 17 Comparison of Predicted and Measured Lift and Drag Increments due to Flap Deflections for a 60 Degree Delta Wing